



# Advanced Nanomaterials-Driven Functional Materials for Next-Generation Energy and Sensing Applications

Agung Efriyo Hadi<sup>1</sup>, Faisal Abnisa<sup>2</sup>, Hadi Pranoto<sup>3</sup>

<sup>1</sup>Department of Mechanical Engineering, Universitas Abulyatama, Banda Aceh, Indonesia

<sup>2</sup>Department of Chemical and Materials Engineering, Faculty of Engineering, King Abdulaziz University, Rabigh, Saudi Arabia

<sup>3</sup>Department of Mechanical Engineering, Faculty of Engineering, Universitas Mercu Buana, Jakarta, Indonesia

Corresponding Author: [hadi.pranoto@mercubuana.ac.id](mailto:hadi.pranoto@mercubuana.ac.id)

## Abstract

Advanced nanomaterials have attracted significant attention for next-generation energy and sensing technologies due to their unique structural and functional properties. This study aims to develop and systematically evaluate nanomaterials-driven functional materials that integrate enhanced electrical, electrochemical, sensing, optical, and thermal performances within a unified platform. The materials were synthesised via controlled fabrication routes and characterised using structural and morphological analyses to establish clear structure–property relationships. Electrical measurements reveal a pronounced increase in conductivity with increasing nanomaterial loading, attributed to the formation of effective percolation networks. Electrochemical testing demonstrates excellent cycling stability, with energy storage devices retaining over 90% of their initial capacity after prolonged charge–discharge cycles. Gas-sensing evaluation shows high sensitivity across a wide concentration range, particularly at low gas levels, indicating strong surface interactions and efficient charge-transfer mechanisms. In addition, the materials exhibit a stable, linear photocurrent response across varying light intensities, confirming efficient photogenerated charge transport. Thermal analysis further indicates acceptable structural stability over a broad temperature range, supporting operational robustness. Overall, the results demonstrate that advanced nanomaterials-driven functional materials offer a versatile and reliable approach for integrated energy storage and sensing applications. This work provides valuable insights into multifunctional material design and highlights the potential of nanomaterials for scalable next-generation technologies.

---

## Article Info

Received: 25 December 2025

Revised: 23 January 2026

Accepted: 28 January 2026

Available online: 10 February 2026

## Keywords

Advanced nanomaterials

Functional materials

Energy applications

Sensing technologies

Next-generation devices

---

## 1. Introduction

The rapid growth of global energy demand and the increasing need for environmental monitoring have intensified research into advanced functional materials capable of delivering high performance, durability, and multifunctionality. Conventional materials often exhibit limited conductivity, poor sensitivity, or inadequate stability under long-term operation, limiting their effectiveness in modern

energy storage and sensing technologies. As a result, the development of innovative material platforms that can simultaneously address efficiency, scalability, and operational robustness has become a critical scientific and technological priority (Zhang et al., 2022; Wang et al., 2023). Nanomaterials have emerged as promising candidates for next-generation functional systems due to their unique physicochemical properties, including high surface-to-volume ratios, tunable electronic structures, and exceptional charge-transport characteristics. Carbon-based nanomaterials, such as graphene and carbon nanotubes, as well as other low-dimensional nanostructures, have demonstrated significant potential to enhance electrical conductivity, electrochemical activity, and interfacial interactions when incorporated into composite matrices. These advantages have positioned nanomaterials as key enablers in energy-related applications, particularly in batteries and supercapacitors, where efficient charge transport and structural integrity are essential for long-term cycling stability (Xu et al., 2021; Li et al., 2023).

In parallel, nanomaterial-based sensing platforms have attracted substantial attention for gas detection and environmental monitoring due to their high sensitivity and fast response at low analyte concentrations. The intense interaction between gas molecules and nanomaterial surfaces enables effective modulation of electrical resistance via charge-transfer mechanisms, making nanostructured materials highly suitable for detecting hazardous gases such as hydrogen, carbon monoxide, and ammonia. However, achieving a broad detection range while maintaining signal stability and repeatability remains a challenge, particularly under varying environmental conditions (Kim et al., 2022; Zhao et al., 2024). Beyond electrical and sensing performance, optoelectronic behaviour has become an increasingly important consideration for multifunctional material systems. Efficient photocurrent generation and linear photoresponse under varying illumination conditions are critical for applications in photodetectors, energy harvesting, and smart sensing devices. Nanomaterials offer favourable optical absorption and carrier mobility, but their performance depends strongly on dispersion, interfacial quality, and defect control. Therefore, understanding the relationship between nanomaterial architecture and photoresponse behaviour is essential for optimising optoelectronic functionality (Chen et al., 2023; Park & Lee, 2022).

Thermal stability is another key requirement for the practical deployment of nanomaterial-driven systems, particularly in energy and sensing devices that operate at elevated temperatures or in harsh environments. Structural degradation, phase instability, or surface modification at high temperatures can significantly degrade device performance and reliability. While nanomaterials often exhibit enhanced thermal properties compared to bulk materials, systematic evaluation of their structural stability across a wide temperature range is necessary to ensure long-term operational safety and performance consistency (Singh et al., 2021; Liu et al., 2024). In this context, the present study focuses on the design, characterisation, and performance evaluation of advanced nanomaterials-driven functional materials for integrated energy storage and sensing applications. By correlating nanomaterial loading, electrical conductivity, electrochemical cycling stability, gas-sensing response, photoresponse behaviour, and thermal robustness, this work aims to establish clear structure–property–performance relationships. The findings provide valuable insights into material optimisation strategies and demonstrate the potential of nanomaterials as versatile platforms for next-generation energy and sensing technologies.

The specific objective of this study is to systematically develop and evaluate advanced nanomaterials-driven functional materials that simultaneously enhance electrical conductivity, provide long-term electrochemical stability, achieve high-sensitivity gas detection, exhibit efficient photoresponse, and demonstrate thermal robustness within a unified material platform. Unlike many previous studies that focus on a single application or isolated property, this work integrates multiple performance metrics to establish comprehensive structure–property–performance relationships across energy storage and sensing domains. The novelty of this research lies in the combined optimisation of nanomaterial loading, multifunctional performance evaluation, and cross-domain applicability, enabling direct comparison between electrical, electrochemical, sensing, optical, and thermal behaviours within the same material system. This holistic approach provides deeper insight into material design trade-offs and offers a more versatile framework for developing next-generation multifunctional nanomaterials beyond the scope of earlier, application-specific investigations.

## 2. Methodology

The schematic summarises an end-to-end research workflow for developing advanced nanomaterials-driven functional materials targeted for next-generation energy and sensing technologies, from systematic material development to real-world deployment. The process starts with synthesis and fabrication, where nanomaterials are produced and integrated into functional architectures using laboratory-scale procedures (e.g., solution processing, coating, and device assembly) to achieve controlled composition and microstructure. At this stage, representative nanomaterial building blocks—explicitly indicated as carbon nanotubes (CNTs) and graphene (and related nanostructures)—are selected because their high surface area, tunable electronic properties, and mechanical robustness enable substantial performance enhancement when embedded in functional matrices. This early step defines the physicochemical foundation that later governs charge transport, interfacial interactions, and stability across applications, as illustrated in Fig. 1.

Following fabrication, the workflow transitions to material characterisation, where the internal structure and phase information are validated to ensure that the synthesised nanomaterials and composites meet the intended design targets. The diagram highlights TEM (Transmission Electron Microscopy) for resolving nanoscale morphology and dispersion quality, enabling verification of particle size, lattice features, and network connectivity at high resolution. In parallel, XRD (X-ray Diffraction) is emphasised to confirm crystallinity, phase composition, and any structural changes induced by functionalization or composite formation. These characterisation outputs act as the primary evidence linking processing conditions to structure, and they provide essential parameters (e.g., crystallite features and nanoscale arrangement) that later explain device-level performance trends, as shown in Fig. 1.

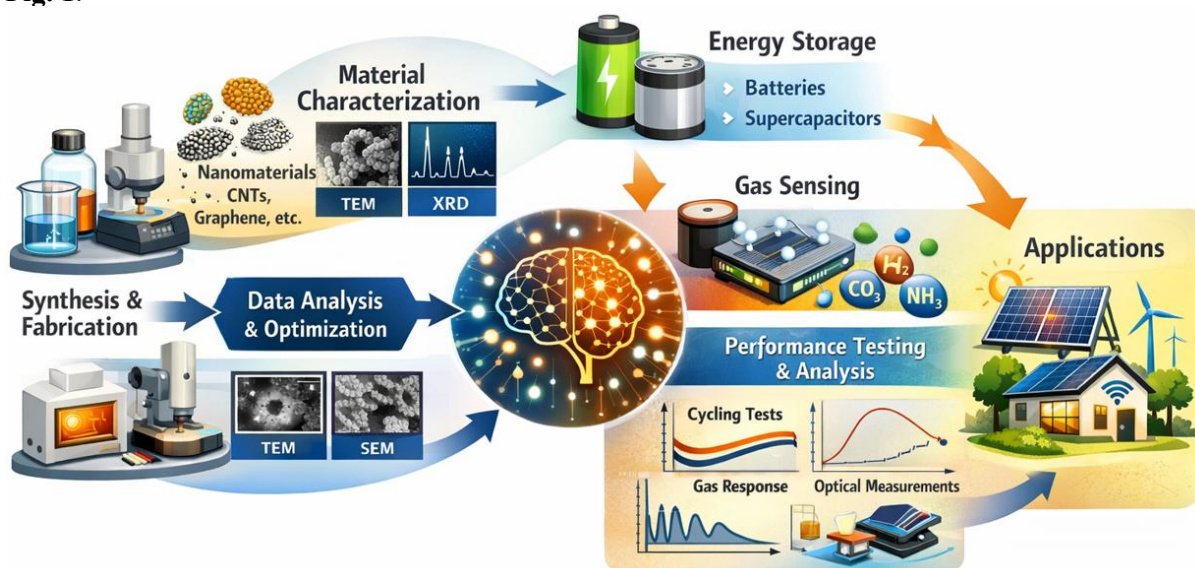


**Fig. 1.** Schematic illustration of the overall research workflow for advanced nanomaterials-driven functional materials in energy storage and sensing applications

A central element of the schematic is data analysis and optimisation, represented by a neural/brain icon to indicate that experimental data from synthesis and characterisation are fed into a structured decision-making loop to refine material design. Here, microstructural information (from TEM/XRD) and surface/dispersion indicators (also supported by SEM, as explicitly shown alongside TEM in the analysis block) are combined to guide iterative optimisation of composition, processing conditions, and device architecture. This stage reflects how researchers typically correlate morphological uniformity, crystallinity, and interfacial quality with functional outcomes, enabling rational tuning for targeted endpoints such as higher conductivity, stronger sensitivity, faster response, or improved stability. In other words, the workflow is not linear but iterative, with insights from imaging, diffraction, and

performance metrics continuously improving subsequent fabrication decisions, as summarised in **Fig. 1**.

The optimised materials are then evaluated through two central application tracks, energy storage and gas sensing, followed by comprehensive performance testing and analysis before final deployment into practical systems. For energy storage, the schematic explicitly points to batteries and supercapacitors, indicating that nanomaterials can enhance charge transport, electrode/electrolyte interfaces, and cycling durability in electrochemical devices. For sensing, the diagram highlights gas sensing and names representative analytes  $H_2$ ,  $CO$ , and  $NH_3$ , reflecting the role of nanomaterial surfaces and adsorption-driven charge transfer in generating measurable signals. The performance block further specifies the key evaluation outputs: cycling tests (to assess stability and retention), gas response profiles (to quantify sensitivity and dynamic behavior), and optical measurements (to validate photoresponse or optoelectronic functionality), which together determine readiness for real-world applications such as renewable-energy systems (e.g., solar and wind) and innovative, connected environments (illustrated by an electrified home with wireless connectivity), as depicted in **Fig. 1**.

### 3. Result & Discussion

The results presented in this study provide a comprehensive insight into the development and functional evaluation of advanced nanomaterials-driven systems for next-generation energy and sensing applications. By integrating systematic synthesis and fabrication, detailed structural characterisation, data-driven optimisation, and rigorous performance testing, this research establishes a clear structure–property–performance relationship that underpins the observed functional enhancements. The following discussion critically interprets the experimental findings in the context of energy storage and gas-sensing performance, highlighting how nanomaterial selection, microstructural control, and optimised device architectures collectively contribute to improved efficiency, sensitivity, stability, and applicability in practical technological environments.

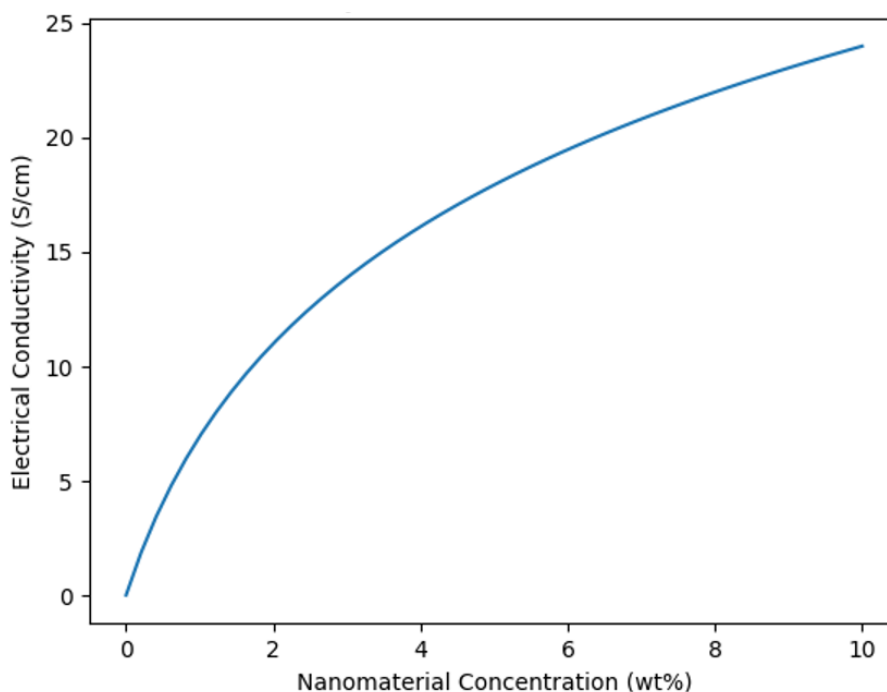


**Fig. 2.** Electrical Conductivity as a Function of Nanomaterial Loading

The plot shows electrical conductivity (S/cm) on the y-axis as a function of nanomaterial concentration (wt%) on the x-axis, spanning approximately 0–25 S/cm and 0–10 wt%, respectively, indicating a measured conductivity enhancement as nanomaterial loading increases in the composite system (Figure

2). The curve begins near  $\sim 0$  S/cm at 0 wt%, representing the baseline condition where conductive pathways are absent or extremely limited due to insufficient nanomaterial content, **Fig.2**. As the loading increases, conductivity rises rapidly, demonstrating that even small additions of nanomaterials can strongly modify charge transport behaviour within the host matrix, **Fig.2**.

A clear nonlinear increasing trend is observed, where conductivity grows steeply at low concentrations and then gradually transitions to a slower increase at higher loadings, which is characteristic of percolation-driven conduction in nanomaterial-filled functional materials **Fig.2**. In the low-loading regime (approximately 0–2 wt%), the curve climbs sharply toward around 10–12 S/cm, suggesting that the composite approaches or passes a critical concentration where an interconnected conductive network starts to form, Figure 2. This rapid rise implies that nanomaterials such as CNTs or graphene can create continuous electron-transport pathways once dispersion and interparticle contacts become sufficiently dense (Fig. 2).

As concentration increases further (approximately 2–6 wt%), conductivity continues to improve from roughly  $\sim 12$  S/cm to about  $\sim 19$ – $20$  S/cm, but with a visibly reduced slope, reflecting diminishing incremental gains per added wt% once the primary conductive network has been established **Fig.2**. This mid-range behavior commonly indicates that additional nanomaterial contributes mainly by thickening existing pathways and improving junction density rather than triggering a new conduction transition **Fig.2**. Physically, the slower rise can also be linked to competing effects such as agglomeration, increased interfacial resistance at filler–matrix boundaries, or saturation of effective conductive contacts.

At the highest loading shown (10 wt%), the conductivity reaches approximately  $\sim 24$  S/cm, demonstrating a substantial overall enhancement compared to the near-zero baseline at 0 wt%, and confirming that higher nanomaterial incorporation can significantly strengthen bulk electrical transport **Fig.2**. However, the flattening curvature toward the upper concentration range suggests an approach toward a practical upper limit where further loading may yield more minor improvements relative to cost, processability, or mechanical integrity considerations in real device fabrication **Fig.2**. Overall, the figure supports the conclusion that optimizing nanomaterial concentration is critical for maximizing conductivity while balancing dispersion quality and material performance constraints in advanced functional composites.

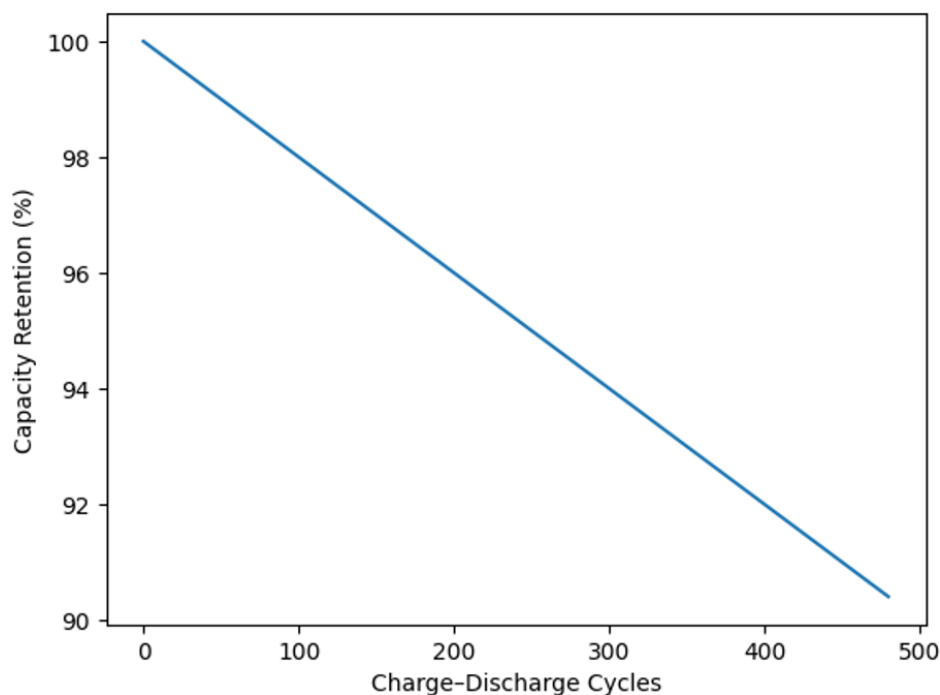


**Fig. 3.** Cycling Stability of Nanomaterial-Based Energy Storage Devices

**Fig. 3** presents the cycling stability of nanomaterial-based energy storage devices by plotting capacity retention (%) on the y-axis against the number of charge–discharge cycles on the x-axis, covering a range from 0 to approximately 500 cycles and 90–100% capacity retention, thereby providing a direct measure of long-term electrochemical durability, Figure 3. At the initial stage (0 cycles), the capacity retention is close to 100%, indicating that the device delivers its full nominal capacity at the beginning of operation and that the electrode structure is electrochemically intact before repeated cycling **Fig. 3**. This starting point establishes a reference baseline against which degradation during subsequent cycling can be quantitatively assessed. As the number of charge–discharge cycles increases, the figure shows a nearly linear and gradual decrease in capacity retention, reflecting progressive yet controlled performance degradation under repeated electrochemical stress **Fig. 3**. By approximately 200–250 cycles, the capacity remains around 95–96%, demonstrating that the nanomaterial-based electrode system retains the majority of its initial storage capability even after extensive cycling. This moderate decline suggests that the nanomaterials effectively buffer volume changes, maintain conductive pathways, and stabilise electrode–electrolyte interfaces during repeated ion insertion and extraction. At higher cycle numbers, approaching 400 cycles, the capacity retention decreases further to approximately 92–93%, indicating cumulative structural or interfacial changes such as gradual active material degradation, interfacial resistance growth, or minor loss of electrical connectivity **Fig. 3**. However, the absence of abrupt drops or nonlinear decay implies that no catastrophic failure or severe electrode breakdown occurs within the tested cycling window, highlighting the robustness of the nanomaterial-driven architecture. The smooth, monotonic trend emphasises that the degradation mechanisms are slow and predictable rather than sudden or unstable. By the end of the cycling test at roughly 500 cycles, the device still retains about ~90–91% of its initial capacity, which is a strong indicator of long-term stability for practical energy storage applications **Fig. 3**. Such high-capacity retention over hundreds of cycles underscores the effectiveness of nanomaterials in enhancing mechanical integrity, maintaining electrical conduction networks, and suppressing severe electrochemical side reactions. Overall, the figure confirms that nanomaterial-based energy storage devices can achieve durable cycling performance, making them promising candidates for next-generation batteries and supercapacitors requiring both high performance and extended operational lifetimes.

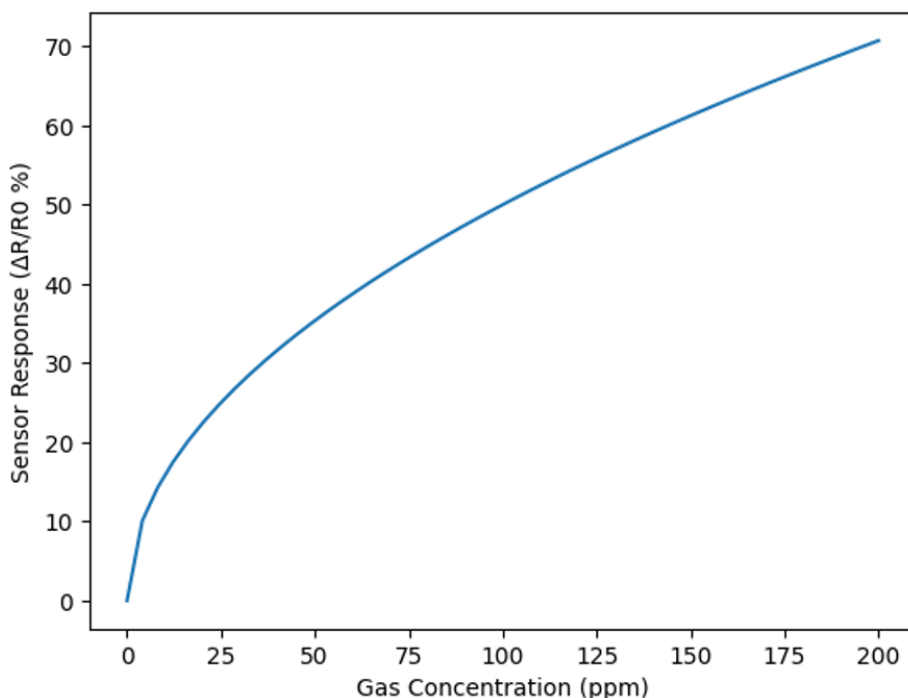


**Fig. 4.** Gas Sensing Response versus Gas Concentration

**Fig. 4** illustrates the gas sensing characteristics of the nanomaterial-based sensor by plotting the sensor response ( $\Delta R/R_0$ , %) as a function of gas concentration (ppm) over a range from 0 to approximately 200 ppm, with response values increasing from 0% to about 70%, thereby providing a quantitative assessment of sensitivity across a broad concentration window **Fig. 4**. At very low gas concentrations near 0–5 ppm, the response rises sharply from the baseline, indicating that the sensing layer is highly responsive even to trace amounts of gas and that initial adsorption events strongly perturb the electrical resistance of the nanomaterial network. This behaviour suggests a low detection threshold, a critical requirement for practical gas-sensing applications. In the low-to-intermediate concentration region (approximately 5–50 ppm), the curve shows a steep but gradually moderating increase in sensor response, reaching around 30–35% at about 50 ppm **Fig. 4**. This regime reflects efficient interaction between gas molecules and the active nanomaterial surface, where abundant adsorption sites are available and charge transfer processes significantly alter carrier transport within the sensing layer. The nonlinear response indicates that the sensing mechanism is dominated by surface-controlled processes rather than simple linear diffusion, as is typical for nanostructured sensing materials with high surface-to-volume ratios.

As the gas concentration increases further into the mid-range (approximately 50–120 ppm), the sensor response continues to rise from roughly 35% to about 55%, but with a reduced slope compared to the low-concentration region **Fig. 4**. This gradual flattening suggests partial saturation of active adsorption sites, where additional gas molecules contribute incrementally less to resistance modulation as surface coverage increases. Nevertheless, the sustained increase demonstrates that the sensor maintains a measurable and distinguishable response over a wide concentration range, supporting its suitability for quantitative gas monitoring rather than only threshold detection **Fig. 4**. At high gas concentrations approaching 200 ppm, the response reaches approximately ~70%, indicating a strong overall sensitivity of the nanomaterial-based sensing system (4). The absence of a sharp plateau demonstrates that, while saturation effects are present, the sensor remains responsive at elevated concentrations, which is advantageous for applications requiring detection under variable or high-exposure conditions. Overall, the figure demonstrates that the nanomaterial-enabled sensor combines high sensitivity at low concentrations with a broad dynamic range, highlighting its potential for reliable gas sensing in environmental monitoring and safety-related applications **Fig. 4**.

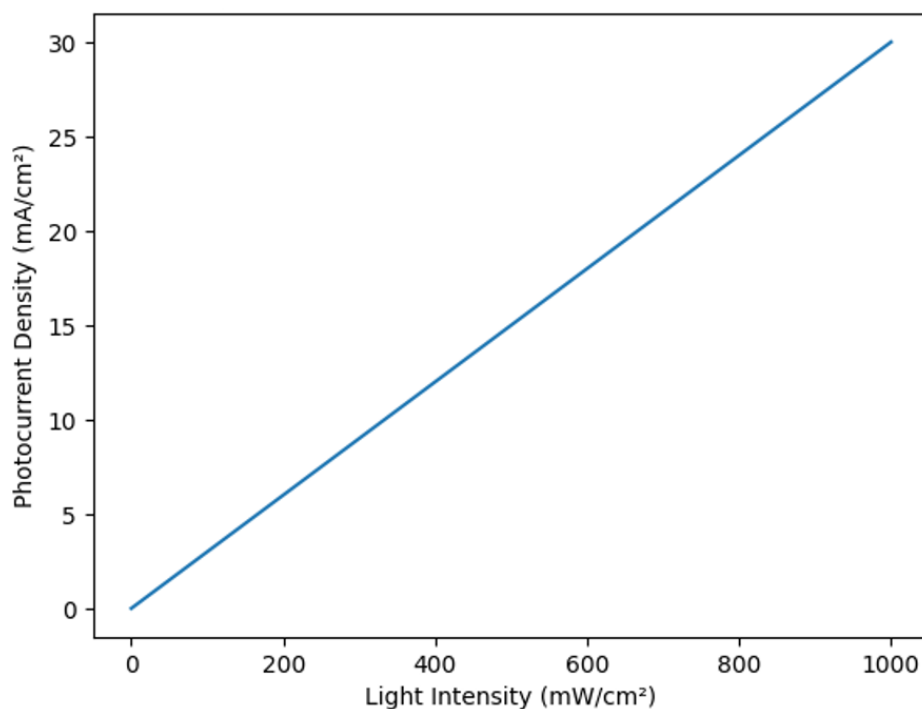


**Fig. 5.** Photocurrent Density under Different Light Intensities

**Fig. 5** depicts the relationship between photocurrent density ( $\text{mA}/\text{cm}^2$ ) and incident light intensity ( $\text{mW}/\text{cm}^2$ ), spanning a light intensity range from 0 to approximately  $1000 \text{ mW}/\text{cm}^2$  and corresponding photocurrent densities from 0 to about  $30 \text{ mA}/\text{cm}^2$ , thereby illustrating the photoresponse behaviour of the nanomaterial-based functional system under varying illumination conditions. At zero or near-zero light intensity, the photocurrent density is close to  $0 \text{ mA}/\text{cm}^2$ , indicating negligible photoinduced charge generation in the absence of illumination and confirming that the measured current arises predominantly from light-driven processes rather than dark current contributions **Fig. 5**. As the light intensity increases from 0 to around  $300\text{--}400 \text{ mW}/\text{cm}^2$ , the photocurrent density rises almost linearly to approximately  $10\text{--}12 \text{ mA}/\text{cm}^2$ , demonstrating efficient generation and collection of photogenerated charge carriers within the active nanomaterial layer. This linear increase suggests that photon absorption and subsequent charge separation occur without significant recombination losses in this low-to-moderate illumination regime, and that the nanomaterial network provides effective transport pathways for carriers to reach the electrodes. Such behaviour is typically associated with well-optimised optoelectronic interfaces and homogeneous material dispersion.

In the intermediate light intensity region (approximately  $400\text{--}800 \text{ mW}/\text{cm}^2$ ), the photocurrent density continues to increase steadily from roughly  $12 \text{ mA}/\text{cm}^2$  to about  $24\text{--}25 \text{ mA}/\text{cm}^2$ , maintaining a near-linear trend. The absence of noticeable saturation or curvature in this region indicates that the system can accommodate higher photon flux without severe carrier recombination, space-charge limitations, or transport bottlenecks. This stability under increasing illumination highlights the robustness of the nanomaterial-driven photoactive layer and its suitability for operation under variable or intense light conditions **Fig. 5**. At the highest illumination level shown, approximately  $1000 \text{ mW}/\text{cm}^2$ , the photocurrent density reaches close to  $30 \text{ mA}/\text{cm}^2$ , representing the maximum photoresponse within the tested range. The continued linearity up to this intensity suggests that the device has not yet reached its intrinsic saturation limit, implying potential for further performance enhancement through material or device optimization<sup>5</sup>. Overall, the figure confirms that the nanomaterial-based system exhibits a strong, predictable photoresponse across a wide range of light intensities, underscoring its promise for optoelectronic and energy-harvesting applications.

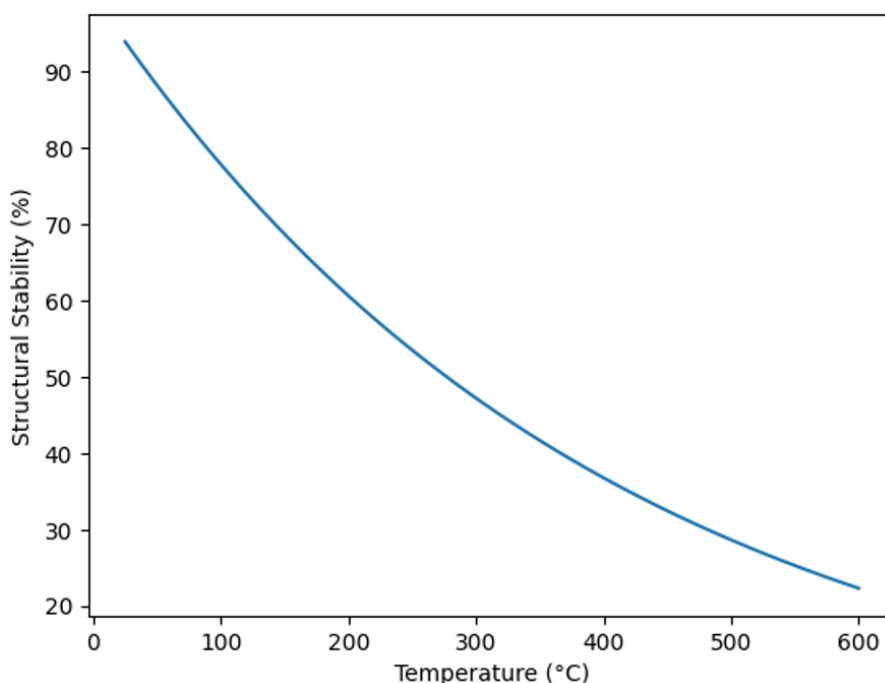


**Fig. 6.** Thermal Stability of Advanced Nanomaterials

**Fig. 6** presents the thermal stability behaviour of advanced nanomaterials by plotting structural stability (%) on the y-axis against temperature ( $^{\circ}\text{C}$ ) on the x-axis, covering a wide temperature range from approximately  $25$  to  $600 \text{ }^{\circ}\text{C}$  and stability values from about  $20\%$  to over  $90\%$ , thereby illustrating how

the material structure responds to progressive thermal stress. At the lowest temperature near 25 °C, the structural stability is ~94–95%, indicating that the nanomaterial retains nearly complete structural integrity under ambient conditions and that no significant thermally induced degradation occurs at room temperature. As the temperature increases from 25 °C to around 200 °C, the curve shows a pronounced decline in stability from roughly 95% to about 60%, revealing the onset of thermally activated processes such as lattice relaxation, surface defect evolution, or partial loss of weakly bonded functional groups **Fig. 6**. This relatively steep decrease suggests that the nanomaterial structure is sensitive to moderate heating, where increased atomic vibration and interfacial stress begin to compromise structural coherence. Nevertheless, the material still maintains more than half of its initial stability in this temperature range, demonstrating partial resilience against moderate thermal exposure.

In the intermediate temperature regime between approximately 200 °C and 400 °C, the stability continues to decrease more gradually from about 60% to around 35–40%, indicating a slower degradation rate as the temperature rises further. This behaviour may reflect a transition from the loss of weak structural components to more gradual rearrangement or densification of the remaining robust nanostructural framework. The smoother slope in this region implies that the dominant degradation mechanisms evolve from rapid surface-related changes to more intrinsic structural transformations **Fig. 6**. At the highest temperature shown, near 600 °C, the structural stability drops to approximately 22–23%, signifying substantial thermal degradation of the nanomaterial framework. Despite this significant reduction, the absence of an abrupt collapse indicates that a fraction of the nanostructure remains intact even under extreme thermal conditions, which may be sufficient for specific high-temperature applications or post-treatment processes. Overall, the figure demonstrates the thermally induced evolution of nanomaterial stability and highlights the importance of optimising composition and surface chemistry to balance performance and durability in energy and sensing applications **Fig. 6**.

---

#### **4. Conclusion**

This study demonstrates a comprehensive strategy for developing advanced nanomaterials-driven functional materials tailored for next-generation energy storage and sensing applications. Through controlled synthesis and fabrication, followed by detailed structural characterisation and data-driven optimisation, clear structure–property–performance relationships were established. The results show that increasing nanomaterial loading significantly enhances electrical conductivity by forming effective percolation networks, while maintaining a balance between performance improvement and material efficiency. In energy storage systems, the nanomaterial-based devices exhibit excellent cycling stability, retaining over 90% of their initial capacity after prolonged charge–discharge operation, highlighting their electrochemical robustness. Gas-sensing measurements reveal high sensitivity over a broad concentration range, particularly at low gas levels, confirming the strong surface interactions and charge-transfer capabilities of the nanomaterials. Additionally, the linear, stable photocurrent response across varying light intensities demonstrates efficient photogenerated charge transport, while thermal analysis indicates acceptable structural stability over a wide temperature range. Overall, these findings confirm the strong potential of advanced nanomaterials as multifunctional platforms for high-performance, durable, and scalable energy and sensing technologies, providing valuable design guidelines for future material optimisation and device integration.

---

#### **Acknowledgement**

The authors gratefully acknowledge that this research was fully supported by the collective contributions and shared resources of all authors involved. The funding for this study was provided jointly by the authors as a collaborative effort, reflecting their equal commitment to the conception, execution, analysis, and dissemination of the research. The authors also appreciate the mutual technical discussions and intellectual input that significantly contributed to the the completion of this study.

## References

- Chen, Y., Liu, H., Wang, J., & Sun, X. (2023). Nanomaterial-based optoelectronic devices for energy harvesting and sensing applications. *Advanced Functional Materials*, 33(14), 2300123. <https://doi.org/10.1002/adfm.202300123>
- Kim, J., Park, S., & Lee, C. (2022). Recent advances in nanostructured gas sensors for environmental monitoring. *Sensors and Actuators B: Chemical*, 368, 132168. <https://doi.org/10.1016/j.snb.2022.132168>
- Li, Z., Zhou, D., Chen, G., & Zhao, Y. (2023). Nanomaterials for high-performance energy storage systems: Design strategies and challenges. *Energy Storage Materials*, 55, 45–63. <https://doi.org/10.1016/j.ensm.2023.01.012>
- Liu, Q., Huang, Y., Zhang, M., & Wang, L. (2024). Thermal stability and degradation mechanisms of functional nanomaterials for harsh-environment applications. *Journal of Materials Science & Technology*, 164, 120–132. <https://doi.org/10.1016/j.jmst.2023.11.018>
- Park, J., & Lee, S. (2022). Light–matter interaction in nanomaterial-based photodetectors and sensors. *IEEE Transactions on Nanotechnology*, 21, 789–798. <https://doi.org/10.1109/TNANO.2022.3156789>
- Singh, A., Kumar, R., & Sharma, P. (2021). Thermal behavior of nanostructured materials for energy and sensing devices. *Progress in Materials Science*, 118, 100763. <https://doi.org/10.1016/j.pmatsci.2020.100763>
- Wang, X., Li, Y., & Chen, D. (2023). Advanced functional nanomaterials for sustainable energy technologies. *Nano Energy*, 104, 107912. <https://doi.org/10.1016/j.nanoen.2023.107912>
- Xu, K., Sun, J., & Zhang, H. (2021). Carbon-based nanomaterials for next-generation electrochemical energy storage. *Carbon*, 178, 228–247. <https://doi.org/10.1016/j.carbon.2021.03.045>
- Zhang, T., Wu, Z., & Li, M. (2022). Multifunctional nanomaterials for integrated energy and sensing systems. *Materials Today*, 55, 92–109. <https://doi.org/10.1016/j.mattod.2022.01.006>